Journal of Engineering Research and Applied Science
Available at www.journaleras.com
Volume 11 (2), December 2022, pp 2062-2077
ISSN 2147-3471 © 2022

Design and Experimental Investigation of Air-Cooled Battery Thermal Management System for Electric Vehicles

Ekrem Sezici, Irfan Cetin, Fikret Polat*

Duzce University, Faculty of Engineering, Mechanical Engineering, Duzce, Turkey.

Accepted 20 November 2022

Abstract

Efforts are made to reduce the biggest problems of climate change by protecting the environment and reducing pollution. 23% of the pollution belongs to the automotive sector. Great efforts are being made to develop electric vehicles (EV) and hybrid electric vehicles (HEV) to replace existing internal combustion engine technology. The battery pack is the largest component of electric and hybrid vehicles. While some or all hybrid electric vehicles are electric, electric vehicles are fully powered by the battery pack. Lithium-ion batteries, which have high energy and power density, are widely used due to their long life and environmental friendliness. However, reduced performance at low and high temperatures, depletion of battery cell durability and life, and safety risks from thermal leaks make a battery thermal management system essential for the battery pack. In this study, a battery pack consisting of 18 cylindrical lithium-ion battery cells and a battery case with three different designs were designed and manufactured. With this structure, cooling experiments of the air-cooled battery thermal management system were carried out. Experiments were first started without using the cooling system. To charge the battery pack, a charge of up to 25.2 volts at a 3-ampere current is provided for 60 minutes. The discharge experiments, which lasted for 20 minutes, were carried out under a load of 327.6 watts. In order to see the effect of air flow rate on cooling, the fan was used at two different speed values. Considering the charge and discharge conditions in three designs; The power consumption of 6 experimental fans was 3.68 watts. The other 6 experiments were carried out with the fan running at a power consumption of 1,984 watts. With the charge and discharge experiments performed without using the cooling system, 14 experiments were completed. All experiments were carried out at room conditions (25 ℃). In order to see the temperature homogeneity in the battery box, the highest and lowest temperature values were examined.

Keywords: Air-Cooled, Battery Thermal Management Systems, Electric Vehicles, Performance

1. Introduction

The average temperature values measured around the world are increasing every year. The main reason for this is the increase of heat-trapping gases in the atmosphere[1], [2]. Carbon dioxide and greenhouse gases are gases that trap heat. This situation is called global warming. Consumption of fossil fuels and gases resulting from industrial and agricultural activities cause global warming. Droughts, floods, unbalanced precipitation, natural disasters such as typhoons and storms are the symptoms of global warming. In order to prevent these disasters, it is necessary to prevent global warming. For this reason, the trend towards alternative energy sources has started and continues to increase day by day[3]–[10]. In 1886, the Benz Patent Motorwagen was the first vehicle to use the revolutionary internal combustion engine [11]. Internal combustion engines, which are still used today, increase global warming with their waste gases. Reasons such as the rapid depletion of fossil fuels and the inability to meet the increasing need have increased the search for alternative energy [12]–[17]. Along with these searches, renewable energy sources are brought to the agenda. Electric and hybrid vehicles are examples of research on this subject.

Electric vehicles work by consuming electrical energy. It contains batteries to store electrical energy. Electric vehicles also have advantages such as reducing environmental pollution, having economical fuel, being easy to use, reducing our dependence on oil countries from which we import. Improvements made on the battery directly affect the performance of the electric vehicle. With this feature, the battery is a very important part in

*Corresponding author:
Phone: +90-541-205-5024, Email: fikretpolat@duzce.edu.tr

electric vehicles. For the battery pack, the heat generated during charge/discharge is a major problem. Overheating of the battery cells in the package may deteriorate and even some cells may lose their function. It is therefore important to maintain the optimum temperature level in the battery pack [18]–[20].

The leading technology of portable power supply, which has become the lifeline of the modern world, is lithium ion technology. The battery pack, which is the most important part of electric and hybrid vehicles, consists of battery cells. Improvements in the power supply in all systems where electricity is used directly affect the performance. This is the reason for the studies on lithium metal. Cooling the battery pack, which heats up due to operation during charging and discharging, or rather keeping it at optimum temperature values for its operation provides better performance.

Heat build-ups when lithium-ion batteries are operating cause temperature rises, causing extensive degradation and shortening of battery life. At the junction points of the electrodes and electrolyte, there is deterioration that will shorten the life of the battery, called battery aging. This also causes a decrease in the capacity of the battery. In the light of research, we can say that for every 10 ℃ increase in temperature, the degradation rate of the battery almost doubles. The high temperature of the battery cell may cause fire or explosion accidents. If the unwanted heat is not removed somehow, it can disrupt the internal structure of the battery cell, and the cell temperature can skyrocket to several hundred degrees in seconds. The separator in a small battery cell can melt and high pressure gases can cause deadly explosion and fire. In addition, the sudden explosion of electrolytes in the battery cell is toxic to human health in closed areas such as car cabins. A reliable, effective cooling system with appropriate equipment and mechanisms is essential to prevent thermal accidents with such devastating effects. For this purpose, battery thermal management systems (BTMS) have emerged and continue to be developed [21]–[24]. Battery thermal management systems are systems that can instantly see the temperature values of the battery that is the power source, activate the existing cooling system when needed, and control the operation of the cooling system. Battery thermal management systems can be grouped under 3 main headings: air-cooled systems, liquid-cooled systems and systems using phase change materials[20], [25]. In this study, air-cooled battery thermal management systems were investigated and a battery pack consisting of 18 cylindrical lithium-ion battery cells and a battery case with three different designs were designed and manufactured. With this structure, cooling experiments of the air-cooled battery thermal management system were carried out.

2. Air-Cooled Battery Thermal Management Systems

Air-cooled systems are simple in construction, do not require cooling cycles and are easy to pack. In addition, air-cooled systems have low maintenance costs and do not pose a risk of liquid leakage into the battery box or electronic parts. Less weight and lower energy consumption are also the biggest advantages of these systems. Air-cooled battery thermal management systems are divided into active cooling and passive cooling systems. In models such as electric and hybrid electric vehicles, with the movement of the vehicle, air flows towards the battery pack, passing between the battery cells and leaving the battery box. The heat energy produced by the battery cells is carried by the air flow. Passive air cooling system is insufficient in cases such as slow movement of the vehicle or high outdoor temperature. Therefore, active cooling is done by adding a fan to increase the air flow. Fans located at the inlet or outlet are used to carry excess heat and to make the temperature distribution more regular. Some of the disadvantages of active cooling systems are the increase in cost, the noise of the fan and the extra energy consumption. In contrast, active air-cooled battery thermal management systems are used for many systems with their reliable performance and overall thermal management as the main cooling strategy. Studies on air-cooled battery thermal management systems generally focus on improvements made in battery box design, cooling channel, air inlet and outlet points, and secondary cooling channel[26]–[28]. There are many studies on air-cooled BTMS in the literature.

Zhang et al proposed a comprehensive optimization scheme that adds secondary outlets and baffle to improve the cooling performance of BTMS. They used computational fluid dynamics (CFD) to investigate the effects of the number and width of secondary outlets and baffles on the cooling performance of BTMS. The authenticity of the CFD method has been verified by the air-cooled heat dissipation experiment of the battery pack [29].

Li et al numerically examined the effect of eighteen airflow configurations to determine an optimized design for the U-type air-cooled BTMS. They

reported that the Reynolds number for the cooler transitions is strongly related to the predicted maximum temperature at the transitions, and that the inlet temperature directly affects the maximum temperature at the cooler transitions, but has less effect on the temperature difference between the transitions[30].

Alharbi and colleagues simulated a battery pack with 45 lithium-ion battery cells. They provided cooling of these cylindrical cells by using air as a coolant in the laminar flow range. They arranged the battery cells in three different ways: diamond, rectangular and triangular. Studies have shown that increasing Re reduces the maximum and average temperature of the battery cells for all three models studied. In addition, the amount of pressure drop increased with increasing Reynolds number for the three settlement models[31].

Ren et al. developed a new type of active air-cooled BTMS based on a U-shaped micro heat pipe array to reduce the temperature rise of the battery cell and improve the temperature uniformity of the battery module during the entire charge and discharge process. They constructed modules with and without U-shaped microtubes for comparative experiments. In the results, they emphasized that the thermal performance of the microtubular active air-cooled BTMS is the best[26].

After the literature review, considering the parameters such as cost, applicability, maintenance and ease of use for battery cells and battery pack, air cooling system is the widely preferred thermal management system, and in this study, the design, manufacturing and experimental investigation of an air-cooled BTMS were carried out.

3. Materials and Method

In the experimental setup created, the air-cooled battery thermal management system was designed and manufactured to allow three different designs. These three designs, which allow air intake from the back and side of the battery pack, are as follows; The model in which the back and sides are open, the model with the back open and the sides closed, and the model with the back closed and the sides open. The characteristics of the battery cell, the creation of the battery pack and the test conditions are detailed in the next sections.

3.1. Battery Pack Design

In this study, the appropriate design for the battery holder and battery pack that will hold the battery cells together was designed using SolidWorks software. Using a 3D printer, the battery holder and the box in which the battery pack will be placed have been produced. The battery holder is shown in Figure 1.

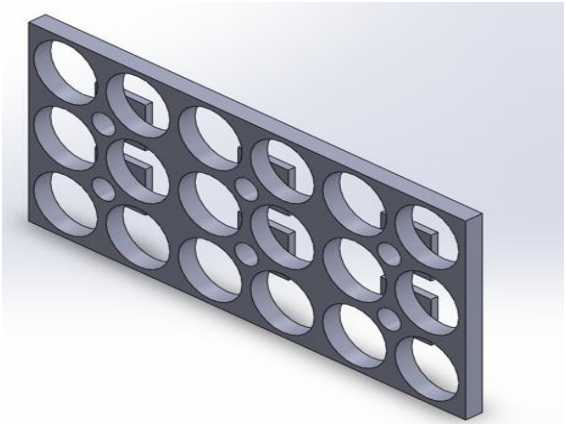

Figure 1. Battery Holder

In order to hold the battery pack, which is formed from cylindrical battery cells, 2 battery holders are produced to be positioned at the top and bottom of the battery cells. Dimensions of the battery holder; The slot diameter is 19 mm, the width is 65 mm, the length is 130 mm, and the thickness is 5 mm.
As seen in Figure 2, sensor input points are designed for the cables that will provide the connection between the temperature sensors and Arduino.

The battery box is designed in such a way that both the batteries and the fan to be used for cooling are kept together. Dimensions of the battery box; width 80 mm, length 140 mm, height 98 mm and wall thickness 3 mm. Figure 3 shows the isometric view of the battery box.

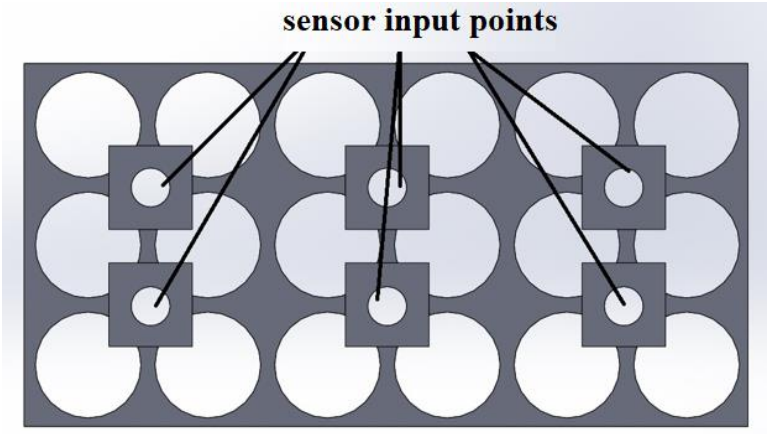

Figure 2. Input Points of Temperature Sensors

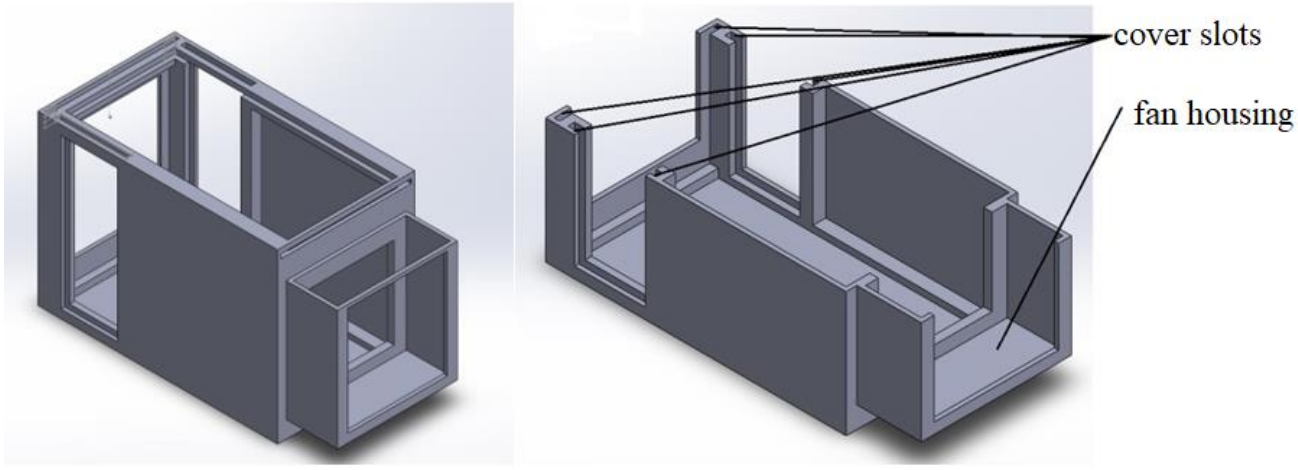

Figure 3. Battery Pack Design Isometric View

In the battery pack, where three different designs come together, each model goes into the battery box – a plug-shaped cover and a slot suitable for these covers are designed. Thanks to the plug-in caps, the battery box is ready for testing for 3 different models. These models can be expressed as:

- Model with open back and closed sides
- Model with closed back and open sides
- Model with open back and sides

While designing the battery pack, a suitable slot for the back cover is designed. Appropriate tolerance has been set to ensure that the cover stays firmly in its seat and prevents unwanted air leakage. For the back cover, an entrance with a width of 2.5 mm and a width of 76.5 mm is specified. The non-perforated rear cover is also designed and manufactured to be used in the model with the back side closed. The dimensions of the two doors, which have a perforated and non-perforated structure, are the same. It is 75.5 mm wide, 91.5 mm long and 2.1 mm thick. The appropriate tolerance for tight closing of the slot and cover is determined as 1 mm and 0.4 mm thickness. The hole diameter of the perforated rear cover is 5 mm.

Covers and slots for these covers are designed on both sides of the battery box, where different designs are combined. The dimensions of the side covers and the dimensions of the side cover rounds are the same. Slot dimensions; It is 41.55 mm long and 3.5 mm thick. The dimensions of the perforated and non-perforated covers are the same and are as follows; width 40.5 mm, height 91.5 mm, thickness 3.1 mm. Considering the side covers and their slots, 0.4 mm thickness and 1 mm width tolerance are determined for a tighter and airtight structure.

After the rear and side covers are placed, the upper cover is designed to cover the upper part of the battery box. Two exit points are determined on the top cover for the cables. The dimensions of the slot made for the top cover in the battery box are as follows; width 76 mm, thickness 3 mm. The dimensions of the top cover are as follows; width 75 mm, length 150 mm, thickness 2.5 mm and hole diameter 8 mm for cable. The top cover and the slot of the cover are determined to be 1 mm in width and 0.5 mm in thickness to ensure tighter interlocking and prevent air leakage.

3.2. Fan and Temperature sensors

In this study, Sunon brand fan with DC feature was used. The fan has dimensions of 60 mm, 60 mm and 15 mm. The fan has a CFM (cubic feet per minute) rating of 17.6 – 30.4.

During the experiment, ds18b20 type temperature sensor was used for monitoring and recording the temperature data. The data obtained from the temperature sensors were recorded in the computer environment via Arduino. The operating range of the temperature sensor is -55 – 125℃. It has an accuracy value of ±0.5 ℃ between -10 ℃ and 85 ℃. The location of the temperature sensors is given in Figure 4.

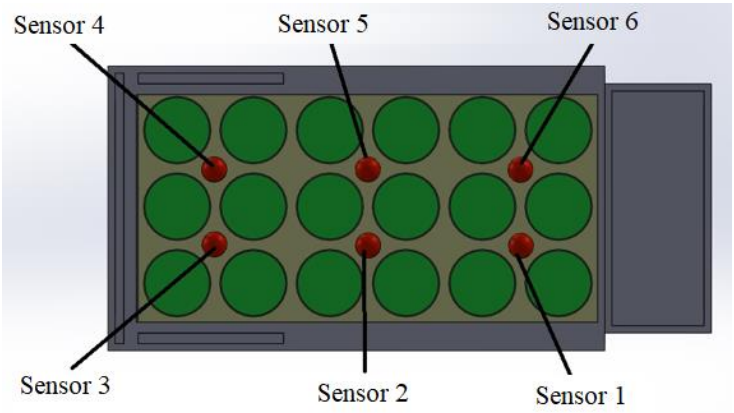

Figure 4. Location of The Temperature Sensors

3.2. Battery Pack Manufacturing

PLA filament was used for the printing process in the 3D printer. A nickel strip is used to provide the electric current between the battery cells, which are stabilized by the battery holder. In order to prevent leakage current and to obtain a safer structure, the connections are covered with insulation tape. A total of 18 batteries are used in the battery pack, and a 6 s (serial) 3 p (parallel) connection has been established. The voltage value taken from the battery pack during discharge is called the nominal value. The nominal voltage of the battery pack is 22.2 volts. The maximum voltage value is 25.3 volts. 18650 Sony VTC 6 lithium-ion battery cells are used to form the battery pack. The technical specifications of these batteries are shown in Table 1.

Table 1. Technical Specifications of 18650 Sony VTC 6 Battery

Voltage	3.7 V
Capacity	3000 mAh
Power	13.69 Wh
Instant Discharge	30 Amper
Weight	48.5 gr
Dimensions	18.25x65 mm

3.2. 3 Different Models in One Box

In air-cooled coil thermal management systems, the air is discharged after circulating through the system. After the box design suitable for the manufactured battery pack, the direction of the air flow should be determined. It is necessary to use more than one battery box in order to investigate the effect of the air flow passing directly between the battery cells and the air flow circulating in the system by entering from the sides of the battery pack on the temperature. Considering that it would be more convenient and easier to have portable surfaces determined on the

box instead of different box models, 3 different battery boxes were obtained as follows.

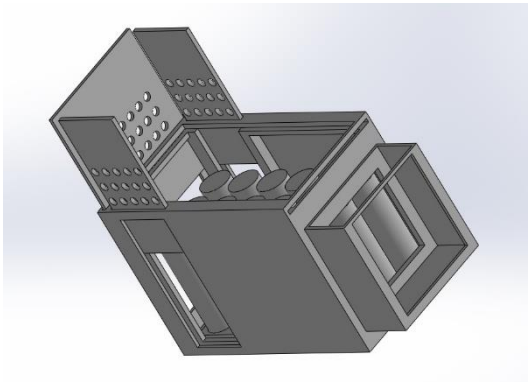

Figure 5. Model with open back and sides

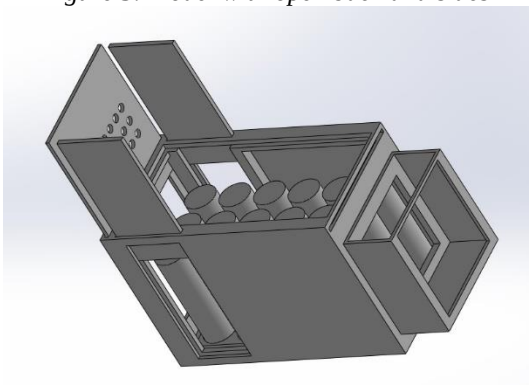

Figure 6. Model with open back and closed sides

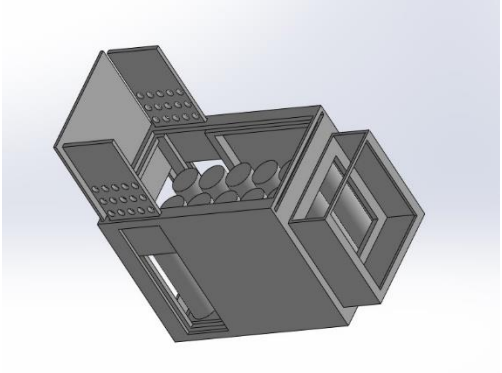

Figure 7. Model with closed back and open sides

3.3. Experimental Setup

The battery cells in the packaged structure are placed in the battery box. As seen in Figure 8, the experimental setup consists of battery cells, battery management system, DC power supply, rheostats, switch, clampmeter, temperature sensors, arduino, computer, fan and cables.

In this study, where three different designs were combined, a 12 V fan was used at two different speeds. In the first case, the fan was operated at 16 V 230 mA. In the second case the fan was operated at 12.4 V and 160 mA current. At these current and voltage values, the fan:

- In the first case where the power consumption is 3.68 Watts; At 6881 rpm, it has 38.86 cubic feet per minute (CFM), which is equivalent to a flow rate of 1.088 m^3/min.
- In the second case where the power consumption is 1.984 Watts; At 5160 rpm, it is equivalent to a flow rate of 0.812 m^3/min with 29.03 cubic feet per minute (CFM). A total of 14 experiments were conducted in fast and slow fan mode for three different designs in charge and discharge conditions.

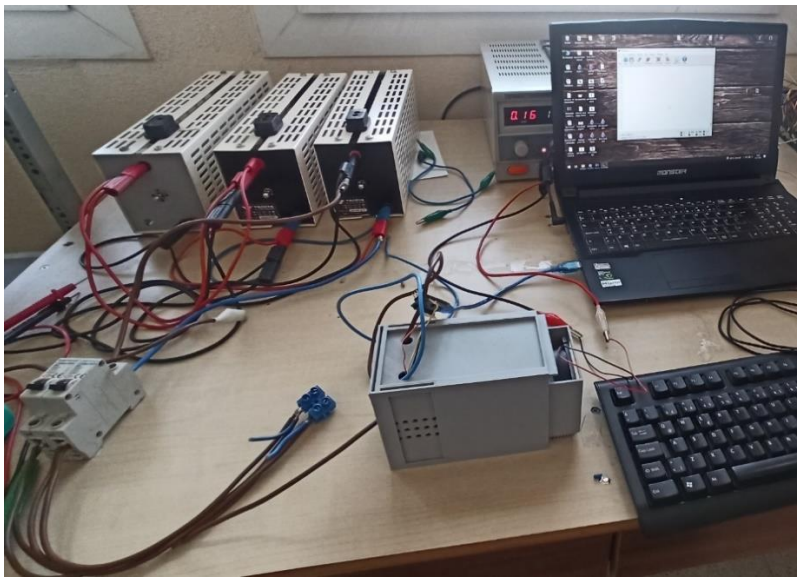

Figure 8. Experimental Setup

In this study, where charging and discharging studies were carried out, DC power source was used to charge the battery pack. In all charging experiments, the charging time was determined as 60 minutes. By connecting 3 rheostats with 500 W power in parallel, the load to be used for the discharge process is distributed equally on the three rheostats. Twenty-minute discharge experiments were carried out with a load of 2.2 Ohm. It has been observed that the current of 11.45 amperes, obtained with a clamp meter from the connection between the rheostat and the battery pack, decreased to 10 amperes after twenty minutes. These experiments, which were carried out between these current and voltage values, which were deemed appropriate for the health and safety of battery cells, were collected in the computer environment.

4. Results and Discussion

Experiments were first started without using the cooling system. To charge the battery pack, a charge up to 25.2 volts at 3 ampere current is provided for 60 minutes. The discharge experiments, which lasted for 20 minutes, were carried out under a load of 327.6 watts. In order to see the effect of air flow rate on cooling, the fan was used at two different speed values. Considering the charge and discharge conditions in three designs; In the case of 6 experimental fans with a power consumption of 3.68 watts, 6 experiments were carried out by operating the fans at a power consumption of 1,984 watts. With the charge and discharge tests performed without using the cooling system, 14 experiments were completed. All experiments were carried out at room conditions (25 ℃). In order to see the temperature homogeneity in the battery box, the highest and lowest temperature values were examined.

4.1. Charge Tests

In the first charging experiment, data were recorded without using the air cooling system. The results obtained are shown in Figure 9. At the end of the 60-minute experiment, the lowest temperature value of the battery cells is 33 °C and the highest temperature value is 34.23 °C. The maximum temperature difference (ΔT) is 1.23 °C.

The time-dependent variation of the temperature of the 6 sensors of the 60-minute charging experiment under 3.68 Watt fan power consumption in the model with the back and sides open is shown in Figure 10.

As can be seen from Figure 10, at the end of the 60-minute experiment, the lowest temperature value of the battery cells is 27.68 °C and the highest temperature value is 28.99 °C. The maximum temperature difference is 1.31 °C.

In the model with the back side open and the sides closed, the time-dependent variation of the temperature of the 6 sensors of the 60-minute charging experiment under 3.68 Watt fan power consumption is shown in Figure 11.

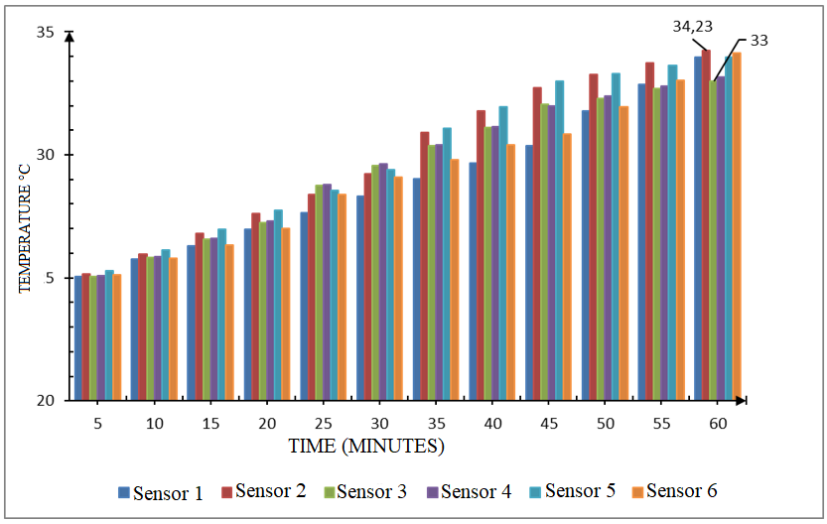

Figure 9. Variation of time-dependent temperature values of the 60-minute charging experiment in which the cooling system is not used

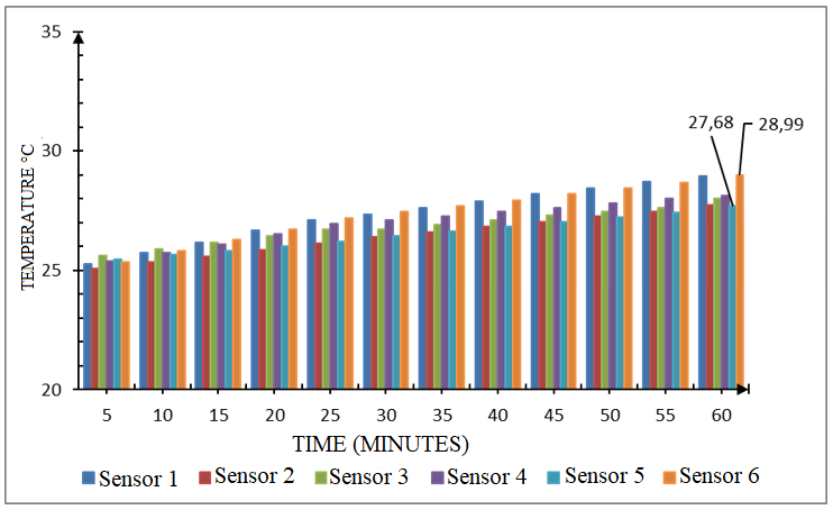

Figure 10. The time-dependent variation of the temperature of the 6 sensors of the 60-minute charging experiment under 3.68 Watt fan power consumption in the model with the back and sides open

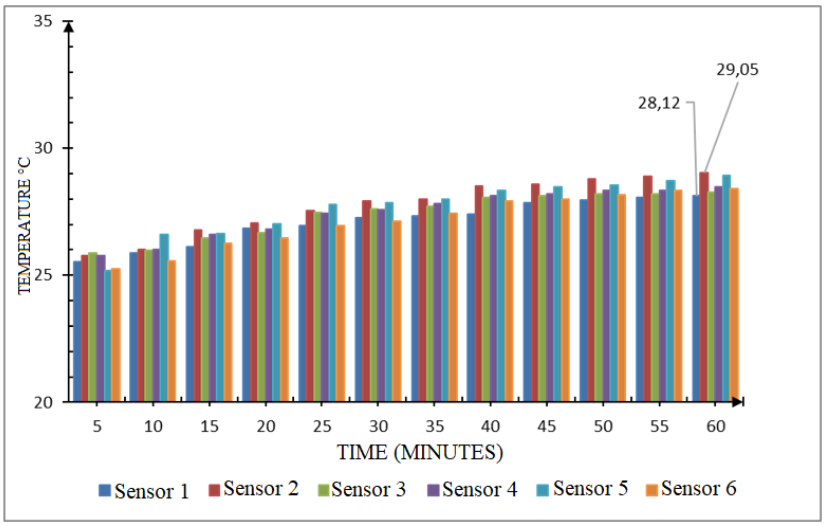

Figure 11. The time-dependent variation of the temperature of the 6 sensors of the 60-minute charging experiment under 3.68 Watt fan power consumption in the model with the back side open and the sides closed

As can be seen from Figure 11, at the end of the 60-minute experiment, the lowest temperature value of the battery cells is 28.12 °C and the highest temperature value is 29.05 °C. The maximum temperature difference is 0.93 °C.

In the model with the back closed and the sides open, the time-dependent variation of the temperature of the 6 sensors of the 60-minute charging experiment under 3.68 Watt fan power consumption is shown in Figure 12.

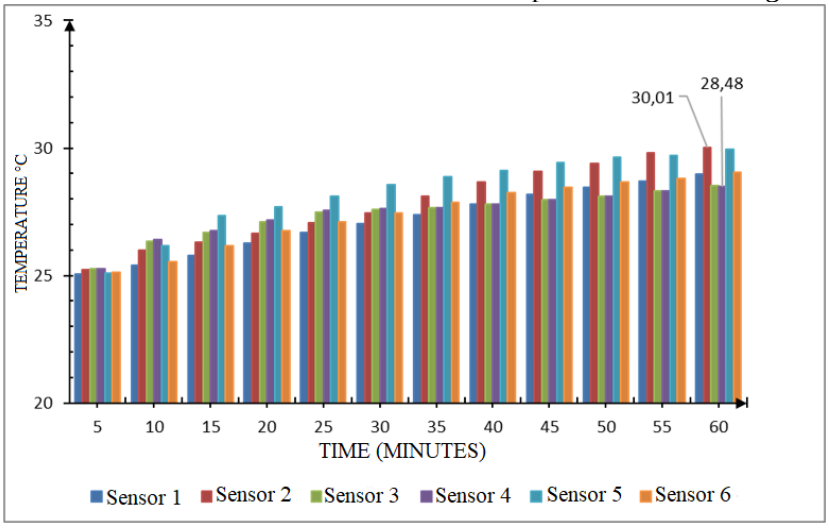

Figure 12. The time-dependent variation of the temperature of the 6 sensors of the 60-minute charging experiment under 3.68 Watt fan power consumption in the model with the back closed and the sides open

As can be seen from Figure 12, at the end of the 60-minute experiment, the lowest temperature value of the battery cells is 28.48 °C and the highest temperature value is 30.01 °C. The maximum temperature difference is 1.53 °C.

The time-dependent variation of the temperature of the 6 sensors of the 60-minute charging experiment under 1.984 Watt fan power consumption in the model with the back and sides open is shown in Figure 13.

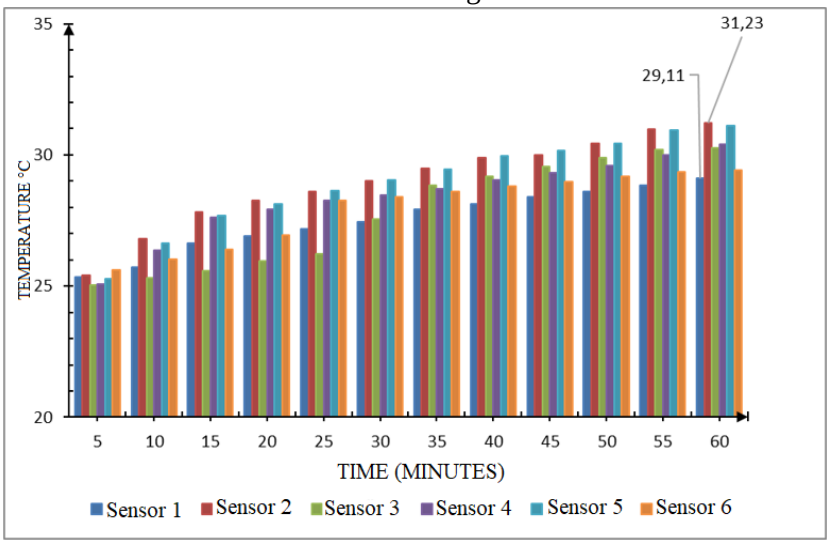

Figure 13. The time-dependent variation of the temperature of the 6 sensors of the 60-minute charging experiment under 1.984 Watt fan power consumption in the model with the back and sides open

As can be seen from Figure 13, at the end of the 60-minute experiment, the lowest temperature value of the battery cells is 29.11 °C and the highest temperature value is 31.23 °C. The maximum temperature difference is 2.12 °C.

In the model with the back side open and the sides closed, the time-dependent variation of the temperature of the 6 sensors of the 60-minute charging experiment under 1.984 Watt fan power consumption is shown in Figure 14.

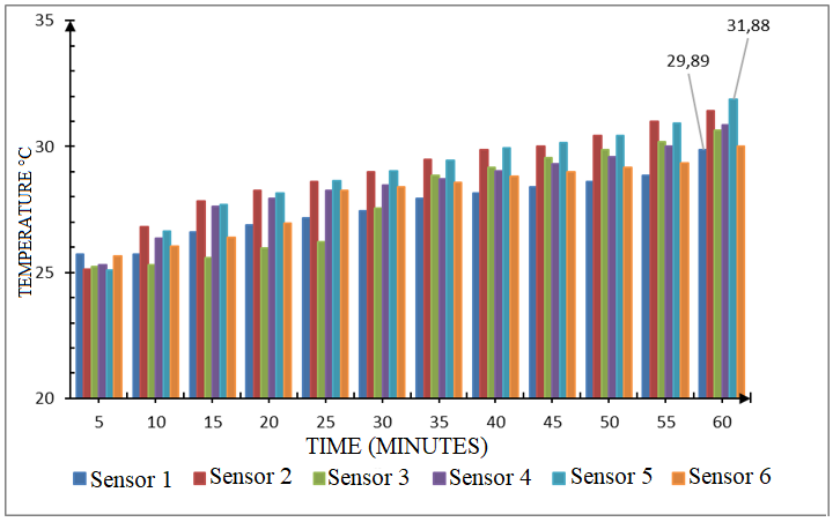

Figure 14. The time-dependent variation of the temperature of the 6 sensors of the 60-minute charging experiment under 1.984 Watt fan power consumption in the model with the back side open and the sides closed

As can be seen from Figure 14, at the end of the 60-minute experiment, the lowest temperature value of the battery cells is 29.89 °C and the highest temperature value is 31.88 °C. The maximum temperature difference is 1.99 °C.

In the model with the back closed and the sides open, the time-dependent variation of the temperature of the 6 sensors of the 60-minute charging experiment under 1.984 Watt fan power consumption is shown in Figure 15.

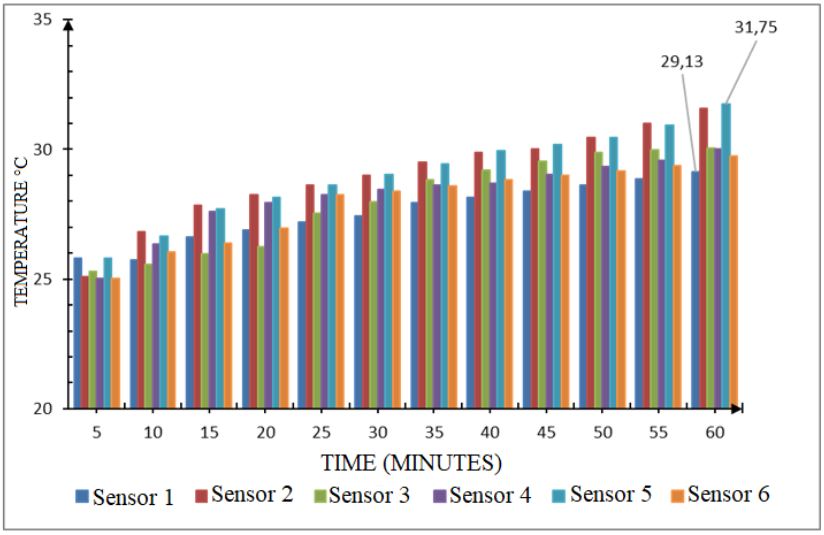

Figure 15. The time-dependent variation of the temperature of the 6 sensors of the 60-minute charging experiment under 1.984 Watt fan power consumption in the model with the back closed and the sides open

As can be seen from Figure 15, at the end of the 60-minute experiment, the lowest temperature value of the battery cells is 29.13 °C and the highest temperature value is 31.75 °C. The maximum temperature difference is 2.62 °C.

4.2. Discharge Tests

When the charging and discharging situations are compared, lithium-ion batteries produce more heat energy in the discharged state. The cooling system was not used in the first discharge test. The time-dependent variation of the temperature of the 6 sensors of the 20-minute discharging experiment is shown in Figure 16.

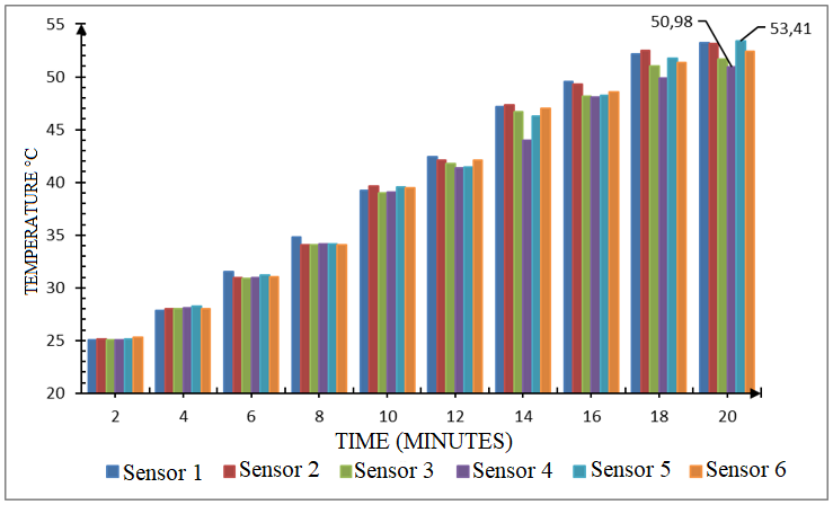

Figure 16. Variation of time-dependent temperature values of the 20-minute discharging experiment in which the cooling system is not used

As can be seen from Figure 16, at the end of the 20-minutes experiment, the lowest temperature value of the battery cells is 50.98 °C and the highest temperature value is 53.41 °C. The maximum temperature difference (ΔT) is 2.43 °C.

In the model with the back and sides open, the time-dependent variation of the temperature of the 6 sensors of the 20-minutes discharging experiment under 3.68 Watt fan power consumption is shown in Figure 17.

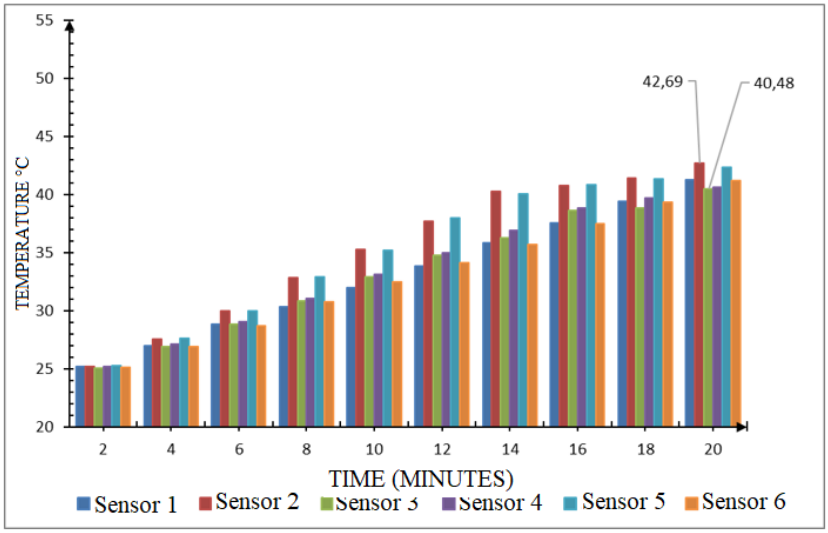

Figure 17. The time-dependent variation of the temperature of the 6 sensors of the 20-minutes discharging experiment under 3.68 Watt fan power consumption in the model with the back and sides open

As can be seen from Figure 17, at the end of the experiment, the lowest temperature value is 40.48 °C and the highest temperature value is 42.69 °C. The maximum temperature difference (ΔT) is 2.21 °C.

In the model with the back side open and the sides closed, the time-dependent variation of the temperature of the 6 sensors of the 20-minutes discharging experiment under 3.68 Watt fan power consumption is shown in Figure 18.

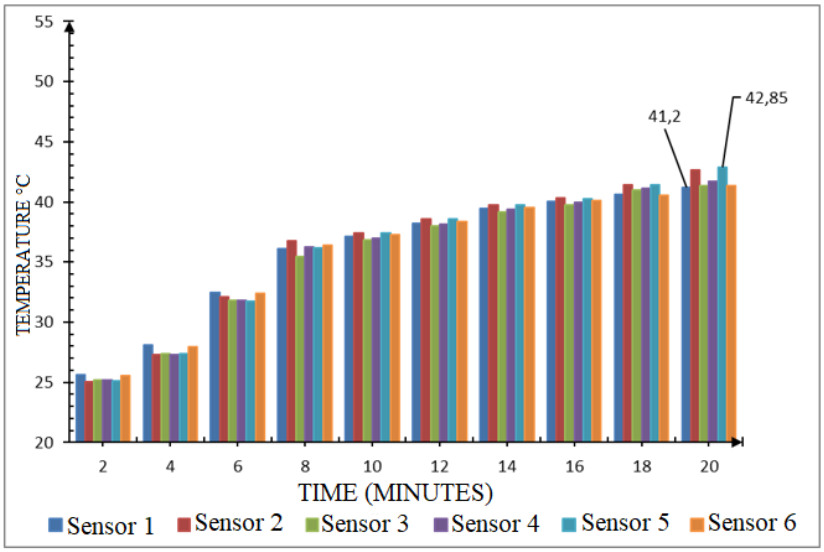

Figure 18. The time-dependent variation of the temperature of the 6 sensors of the 20-minutes discharging experiment under 3.68 Watt fan power consumption in the model with the back side open and the sides closed

As can be seen from Figure 18, at the end of the experiment, the lowest temperature value is 41.2 °C and the highest temperature value is 42.85 °C. The maximum temperature difference (ΔT) is 1.65°C.

In the model with the back closed and the sides open, the time-dependent variation of the temperature of the 6 sensors of the 20-minutes discharging experiment under 3.68 Watt fan power consumption is shown in Figure 19.

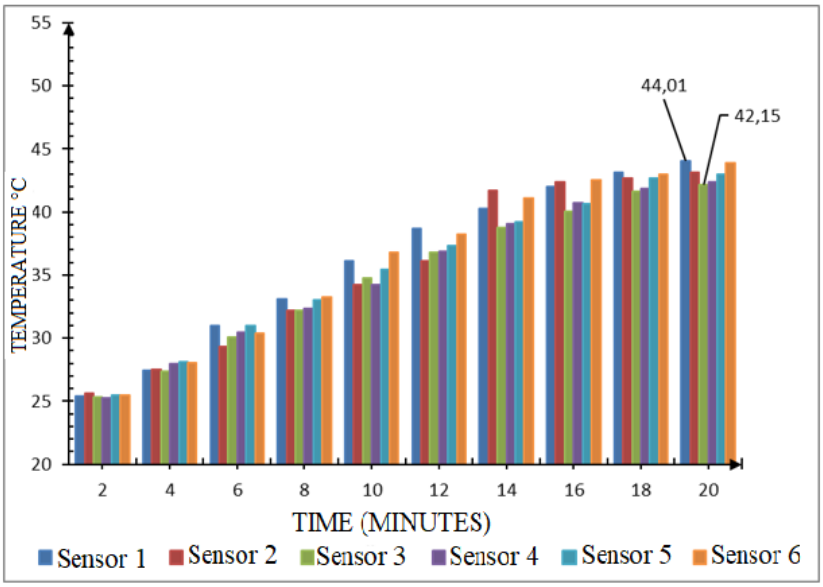

Figure 19. The time-dependent variation of the temperature of the 6 sensors of the 20-minutes discharging experiment under 3.68 Watt fan power consumption in the model with the back closed and the sides open

As can be seen from Figure 19, at the end of the experiment, the lowest temperature value is 42.15 °C and the highest temperature value is 44.01 °C. The maximum temperature difference (ΔT) is 1.86 °C.

In the model with the back and sides open, the time-dependent variation of the temperature of the 6 sensors of the 20-minutes discharging experiment under 1.984 Watt fan power consumption is shown in Figure 20.

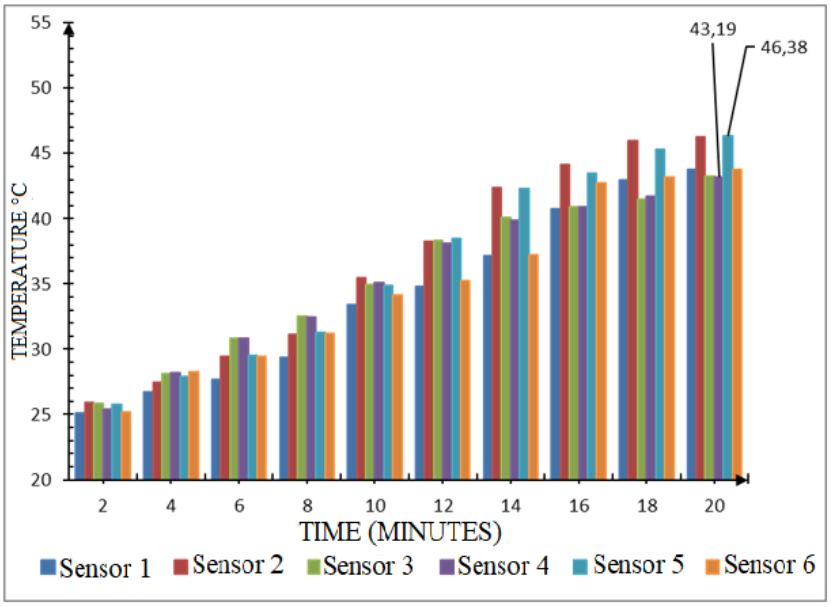

Figure 20. The time-dependent variation of the temperature of the 6 sensors of the 20-minutes discharging experiment under 1.984 Watt fan power consumption in the model with the back and sides open

As can be seen from Figure 20, at the end of the experiment, the lowest temperature value is 43.19 °C and the highest temperature value is 46.38 °C. The maximum temperature difference (ΔT) is 3.19 °C.

In the model with the back side open and the sides closed, the time-dependent variation of the temperature of the 6 sensors of the 20-minutes discharging experiment under 1.984 Watt fan power consumption is shown in Figure 21.

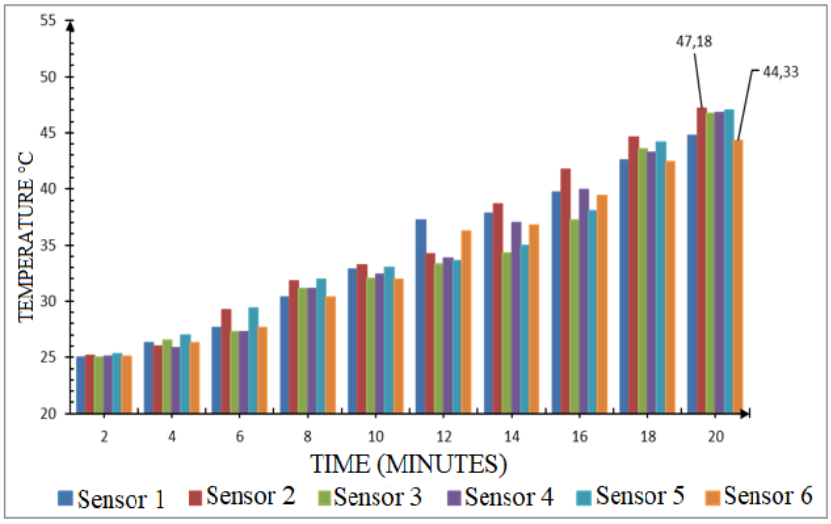

Figure 21. The time-dependent variation of the temperature of the 6 sensors of the 20-minutes discharging experiment under 1.984 Watt fan power consumption in the model with the back side open and the sides closed

As can be seen from Figure 21, at the end of the experiment, the lowest temperature value is 44.33 °C and the highest temperature value is 47.18 °C. The maximum temperature difference (ΔT) is 2.85°C.

In the model with the back closed and the sides open, the time-dependent variation of the temperature of the 6 sensors of the 20-minutes discharging experiment under 1.984 Watt fan power consumption is shown in Figure 22.

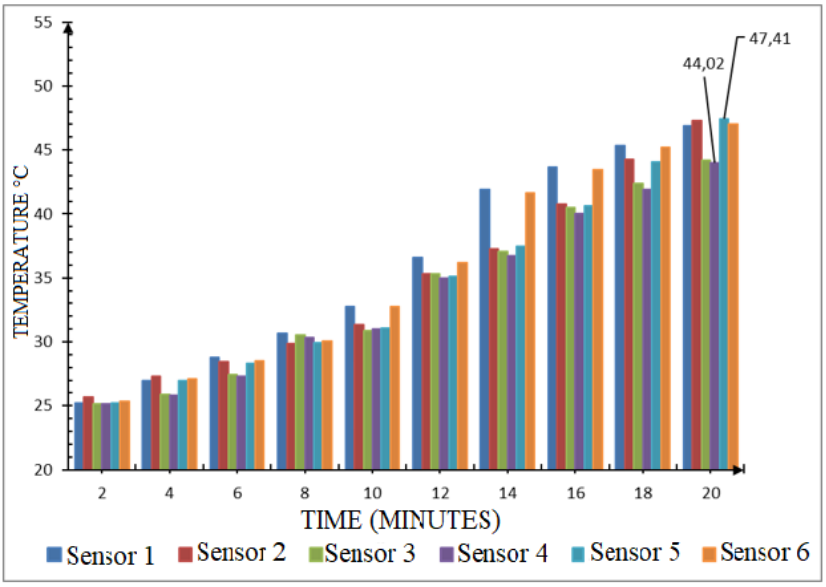

Figure 22. The time-dependent variation of the temperature of the 6 sensors of the 20-minutes discharging experiment under 1.984 Watt fan power consumption in the model with the back closed and the sides open

As can be seen from Figure 22, at the end of the experiment, the lowest temperature value is 44.02 °C and the highest temperature value is 47.41 °C. The maximum temperature difference (ΔT) is 3.39 °C.

5. Conclusions

In this study, a research was conducted on the thermal problems of battery battery packs, which are of great importance in developing electric vehicle technology. Improvement studies on lithium-ion battery cells that make up the battery pack directly affect the performance and cost characteristics of the structure used. The biggest problem of lithium-ion batteries in the battery pack of electric and hybrid vehicles is thermal irregularity. During use, battery cells also generate heat energy. If this heat energy is not kept under control, it causes serious problems. However, the battery battery pack is also adversely affected by low temperature in cold climate conditions. It has been determined that the battery packs need a battery thermal management system in order to maintain their operation at optimum temperature values, and the cooling performance of the air-cooled battery thermal management system has been experimentally investigated. Three battery pack models and two different fan speeds were used in the experiments carried out under room conditions. When the data taken from 6 different temperature sensors are examined, the following inferences are made.

- Fast air flow ensures that the battery pack has a more homogeneous temperature structure,
- The battery cells in the middle of the battery pack produce more heat energy,
- The large air inlet cross-section provides better cooling of the battery pack,
- In the model where the air flows linearly, the back side is open and the sides are closed, the battery cells have a more homogeneous temperature distribution,
- Fast air flow accelerates the cooling process and provides better cooling performance.

5.Acknowledgments

The authors wish to place their sincere thanks to Duzce University Scientific Research Project Coordinatorship for financial support for the Project No: 2022.06.05.1296.

6. References

[1] R. P. Rastogi, A. Pandey, C. Larroche, and D. Madamwar, “Algal Green Energy – R&D and technological perspectives for biodiesel production”, *Renew. Sustain. Energy Rev.*, c. 82, ss. 2946–2969, Şub. 2018.

[2] R. Sindhu, G. Amba Prasad Rao, and K. Madhu Murthy, “Effective reduction of NOx emissions from diesel engine using split injections”, *Alexandria Eng. J.*, c. 57, sayı 3, ss. 1379–1392, Eyl. 2018.

[3] Ü. Ağbulut, F. Polat, and S. Sarıdemir, “A comprehensive study on the influences of different types of nano-sized particles usage in diesel-bioethanol blends on combustion, performance, and environmental aspects”, *Energy*, c. 229, s. 120548, Ağu. 2021.

[4] Ü. AĞBULUT and H. BAKIR, “The Investigation on Economic and Ecological Impacts of Tendency to Electric Vehicles Instead of Internal Combustion Engines”,

Duzce Univ. J. Sci. Technol., c. 7, sayı 1, ss. 25–36, Oca. 2019.

[5] Ü. Ağbulut, M. K. Yeşilyurt, and S. Sarıdemir, "Wastes to energy: Improving the poor properties of waste tire pyrolysis oil with waste cooking oil methyl ester and waste fusel alcohol – A detailed assessment on the combustion, emission, and performance characteristics of a CI engine", *Energy*, c. 222, s. 119942, May. 2021.

[6] Ahmad, T., & Zhang, D. (2020). A critical review of comparative global historical energy consumption and future demand: The story told so far. Energy Reports, 6, 1973-1991.

[7] M. Ali ÖZEL, "Elektrikli Araçlarda Kullanılan Batarya Paketinin Termal Modeli Ve Analizi", 2019.

[8] M. Çeçen, C. Yavuz, C. A. Tırmıkçı, S. Sarıkaya, and E. Yanıkoğlu, "Analysis and evaluation of distributed photovoltaic generation in electrical energy production and related regulations of Turkey", *Clean Technol. Environ. Policy*, c. 24, sayı 5, ss. 1321–1336, Tem. 2022.

[9] İ. Çetin, E. Sezici, M. Karabulut, E. Avci, and F. Polat, "A comprehensive review of battery thermal management systems for electric vehicles", *https://doi.org/10.1177/09544089221123975*, Eyl. 2022.

[10] Y. Maral, M. Aktas, O. Erol, R. Ongun, and F. Polat, "An examinaion about thermal capacities of thermoelectric coolers in battery cooling systems", *J. Eng. Res. Appl. Sci.*, c. 6, sayı 2, ss. 703–710, 2017.

[11] J. Foreman-Peck, "An American and European technological difference: The early motor car power source", *https://doi.org/10.1080/00076791.2019.1590338*, c. 61, sayı 7, ss. 1158–1174, Eki. 2019.

[12] F. Polat, "Performance and emission behaviors of a CI engine fueled by waste feedstocks at varying compression ratios":, *https://doi.org/10.1177/09544089221074845*, Şub. 2022.

[13] M. KILINÇEL, E. TOKLU, and F. POLAT, "Influence of A Novel Catalysis on The Pyrolysis Yields Obtained by Two Different Reactors", *Çanakkale Onsekiz Mart Üniversitesi Fen Bilim. Enstitüsü Derg.*, c. 6, sayı 2, ss. 317–327, 2020.

[14] A. T. Sipra, N. Gao, and H. Sarwar, "Municipal solid waste (MSW) pyrolysis for bio-fuel production: A review of effects of MSW components and catalysts", *Fuel Process. Technol.*, c. 175, sayı November 2017, ss. 131–147, 2018.

[15] Ü. Ağbulut, S. Sarıdemir, U. Rajak, F. Polat, A. Afzal, and T. N. Verma, "Effects of high-dosage copper oxide nanoparticles addition in diesel fuel on engine characteristics", *Energy*, c. 229, s. 120611, Ağu. 2021.

[16] Ü. Ağbulut, "Understanding the role of nanoparticle size on energy, exergy, thermoeconomic, exergoeconomic, and sustainability analyses of an IC engine: A thermodynamic approach", *Fuel Process. Technol.*, c. 225, s. 107060, Oca. 2022.

[17] Ü. Ağbulut, A. E. Gürel, and S. Sarıdemir, "Experimental investigation and prediction of performance and emission responses of a CI engine fuelled with different metal-oxide based nanoparticles–diesel blends using different machine learning algorithms", *Energy*, c. 215, 2021.

[18] S. Tamilselvi *et al.*, "A Review on Battery Modelling Techniques", *Sustain. 2021, Vol. 13, Page 10042*, c. 13, sayı 18, s. 10042, Eyl. 2021.

[19] T. Talluri, T. Kim, K. S.- Energies, and undefined 2020, "Analysis of a battery pack with a phase change material for the extreme temperature conditions of an electrical vehicle", *mdpi.com*.

[20] C. Zhao *et al.*, "Hybrid battery thermal management system in electrical vehicles: A review", *mdpi.com*.

[21] J. Kim, J. Oh, and H. Lee, "Review on battery thermal management system for electric vehicles", *Appl. Therm. Eng.*, c. 149, ss. 192–212, Şub. 2019.

[22] Y. Li *et al.*, "Optimization of thermal management system for Li-ion batteries using phase change material", *Appl. Therm. Eng.*, c. 131, ss. 766–778, Şub. 2018.

[23] R. Jilte, A. Afzal, and S. Panchal, "A novel battery thermal management system using nano-enhanced phase change materials", *Energy*, c. 219, s. 119564, 2021.

[24] J. Shen, Y. Wang, G. Yu, ve H. Li, "Thermal Management of Prismatic Lithium-Ion Battery with Minichannel Cold Plate", *J. Energy Eng.*, c. 146, sayı 1, s. 04019033, Şub. 2020.

[25] M. Subramanian *et al.*, "A technical review on composite phase change material based secondary assisted battery thermal management system for electric vehicles", *J. Clean. Prod.*, c. 322, s. 129079, Kas. 2021.

[26] R. Ren, Y. Zhao, Y. Diao, L. Liang, and H. Jing, "Active air cooling thermal management system based on U-shaped micro heat pipe array for lithium-ion battery", *J. Power Sources*, c. 507, s. 230314, Eyl. 2021.

[27] T. Wang, K. Tseng, J. Z.-A. T. Engineering, ve undefined 2015, "Development of efficient air-cooling strategies for lithium-ion battery module based on empirical heat source model", *Elsevier*.

[28] D. G. Kröger, *Air-cooled Heat exchangers and Cooling Towers: Thermal-Flow Performance Evaluation and Design:V1*, c. 1. 2004.

[29] F. Zhang, P. Liu, Y. He, and S. Li, "Cooling performance optimization of air cooling lithium-ion battery thermal management system based on multiple secondary outlets and baffle", *J. Energy Storage*, c. 52, s. 104678, Ağu. 2022.

[30] X. Li, J. Zhao, J. Yuan, J. Duan, and C. Liang, "Simulation and analysis of air cooling configurations for a lithium-ion battery pack", *J. Energy Storage*, c. 35, s. 102270, Mar. 2021.

[31] K. A. M. Alharbi, G. F. Smaisim, S. M. Sajadi, M. A. Fagiy, H. Aybar, and S. E. Elkhatib, "Numerical study of lozenge, triangular and rectangular arrangements of lithium-ion batteries in their thermal management in a cooled-air cooling system", *J. Energy Storage*, c. 52, s. 104786, Aug. 2022.